

Electrochemical Corrosion of Ferritic 409 and 439 Stainless Steels 409 and 439 in NaCl and H₂SO₄ solutions

C. Gaona Tiburcio¹, F.H. Estupiñán López¹, P. Zambrano Robledo¹, J. A. Cabral M¹, C. Barrios Durtewitz², F. Almeraya Calderón^{1,}*

¹Universidad Autónoma de Nuevo León, UANL. Facultad de Ingeniería Mecánica y Eléctrica, FIME Centro de Investigación e Innovación en Ingeniería Aeronáutica, CIIIA, Carretera a Salinas Victoria Km. 2.3 s/n. Apodaca Nuevo León. 66600 México.

²Universidad Autónoma de Sinaloa Facultad de Ingeniería Mochis, Fuente de Poseidón y Prol. Ángel Flores S/N, Los Mochis, Sinaloa, México.

*E-mail: flameraya.uanl.ciiia@gmail.com

Received: 14 August 2015 / Accepted: 25 November 2015 / Published: 1 January 2016

Over the time the automotive industry has evolved in the use of steels in different parts of vehicles, thanks to the materials technology; a deciding factor in the market are the corrosion properties. Based on this fact, it was decided the incorporation of stainless steels (SS), especially in parts which are exposed to environment, such as exhaust pipes, where the 409 SS tops the production list and in some cases replaced by the 439 SS. This study makes a comparative performance evaluation between ferritic steels 409 and 439, in different electrolytes that are important to automotive industry like 5% brine as simulating saline environment, 3.5% sulfuric acid (H₂SO₄) solution and water as the blank, with the purpose to identify their corrosion behavior. Given the characteristics of stainless steel 409 and 439, is expected pitting, so mechanistic electrochemical techniques are used, such as cyclic potentiodynamic polarization curves and electrochemical noise. The corrosion kinetics indicated that the 439 stainless steel in H₂SO₄ had the highest corrosion rate, while in NaCl the 409 had the highest. Both materials have a pitting corrosion type in sodium chloride using cyclic polarization curves and electrochemical noise techniques for its evaluation.

Keywords: Pitting corrosion, electrochemical noise, cyclic polarization, ferritic stainless steel 409 and 439, Automobile industry.

1. INTRODUCTION

Stainless steels are iron base alloys containing chromium, carbon and other elements, particularly nickel, molybdenum, manganese, silicon and titanium. Chromium, which it is in

a not less than 10% percent, confers the property of being more corrosion resistant than the iron would be without the presence of the alloying [1]. Ferritic stainless steels are used to a greater extent in automotive exhaust components due to their excellent resistance to chloride-induced stress corrosion cracking (SCC), adequate high-temperature strength, good resistance to oxidation and wet corrosion, and sufficient resistance to thermal fatigue [1–4].

The automaker recently industry has been challenged to improve the quality of materials used due to the growing demands of the market and a crucial part of any car is the exhaust pipe, which serves to eject the engine generated combustion gases toward the environment and being its main objective to reduce the pollutant gases from every car. Although it is located in the bottom of the car, is not covered by any structure that could protect it from aqueous medium, thus accelerating the corrosion process of this car part.

The leader material on the market for the manufacture of exhaust pipes is 409 stainless steel and belongs to the family of ferritic steels, which the chromium content are slightly above 10%, are not neither hardened by mechanical work nor heat treating and in some cases only, are magnetic. The ferritic 409 stainless steel contains only 10.5% of chromium [5], which gives corrosion resistance just above any carbon steel and at the same time makes the cheapest stainless steel in the market and the less dense, an important characteristic of exhaust piping.

The 439 stainless steel, as same as 409, belongs to the family of ferritic stainless steels, however this steel contains a higher chromium percentage ranging from 17 to 19%, giving a better corrosion properties; in terms of mechanical performance and density, are alike as SS409 (SS, acronym Stainless Steel). These similar properties, makes it a material that is useful in the application for mufflers.

The main mechanism of corrosion that arises is pitting that eventually affects the good performance of the exhaust pipes. The liquid solution made from melted snow and road salt, the acid rain components and, generally, any type of water in constant contact with the pipe surface, will play a key role in the formation of pits. About electrochemical mechanisms, is known that the pits, positively charged, attracts ions of chlorine, increasing acidity of the solution, then the pH inside the pit decreases until 2 or 3, causing acceleration of the corrosion process, and in presence of chloride, the ions pits are growing by an autocatalytic mechanism [6].

Khedr [7] reported that chloride ions adsorbed on the surface of metals inhibit the reaction of dissolution in 10 N H₂SO₄, but at lower concentrations of sulfuric, the ions of chloride accelerate the dissolution rate as consequence of the formation of pits on the superficial film.

Various electrochemical tests allow to qualitatively assess the tendency of materials to suffer corrosion pitting, the first and to be used in this study, is the technique of cyclic potentiodynamic polarization (CPP), which bounds up the current density with potential, by polarization means; with this technique, it is able to obtain information as pitting potential, rate of corrosion, passivation current, and by analyzing the transpassive region graph it can deduced the sensitivity of the material to develop pitting [8]. Furthermore, the technique of electrochemical noise detects, which is a non-destructive technique that measures fluctuations in potential and current, instantaneous response of the surface change conditions that starts to corrode allowing this method to be a powerful tool for monitoring the corrosion [9].

The present study aims to assess the corrosion resistance of 409 and 439 ferritic stainless steels (for use in exhaust systems environment) in solutions of sodium chloride (NaCl) and sulfuric acid (H_2SO_4) to define the type and corrosion rate; evaluation was performed using cyclic potentiodynamic polarization (CPP) and electrochemical noise (EN). All materials were observed by scanning electron microscopy (SEM) and optical microscopy (OM).

2. EXPERIMENTAL PROCEDURE

The materials used in this study were the stainless steel type AISI 409 and 439. The quantitative chemical analysis was performed using the technique of X-ray fluorescence spectrometry (XRF).

The electrodes were obtained from stainless steel sheets AISI 409 and 439, joined to a bare copper wire at the ends to make the necessary electrical contact on the electrochemical tests and then encapsulated in epoxy resin. The exposed area of the samples in the various solutions was $1cm^2$. The samples were subjected to a grinding process up to a grade 800 silicon carbide; then sprayed ethanol and dried with hot air and pressure. Later the samples were stored in a desiccator for a period of 12 hours prior to the electrochemical test. The electrolyte used in this study were water, 5% brine (NaCl) and 3.5% sulfuric acid (H_2SO_4), the latter products prepared with distilled water and reagent grade.

Electrochemical noise tests were carried out by immersion in a corrosion cell electrodes (3) (two nominally identical working electrodes), and a reference electrode saturated calomel (SCE). Platinum and a counter electrode, was used for testing CPP and EN. Assays were performed at room temperature.

The equipment used was a potentiostat / galvanostat / ZRA "Gill AC 1657". The number of points for each measured was 2048 at a rate point per second, for electrochemical noise [9]. In the cyclic potentiodynamic polarization technique, the sample was polarized from -300 to 1200 mV at a scan rate of 60 mV/min [8]. After the electrochemical tests finished, the samples were dried with ethanol and after dried with pressurized hot air, stored in a desiccator and later performed the optical and scanning electron microscopy (SEM) analysis. Both analyzes were performed on the entire sample surface to identify localized corrosion attack.

The tests were conducted with a repeatability of three samples, however, a single test results are presented.

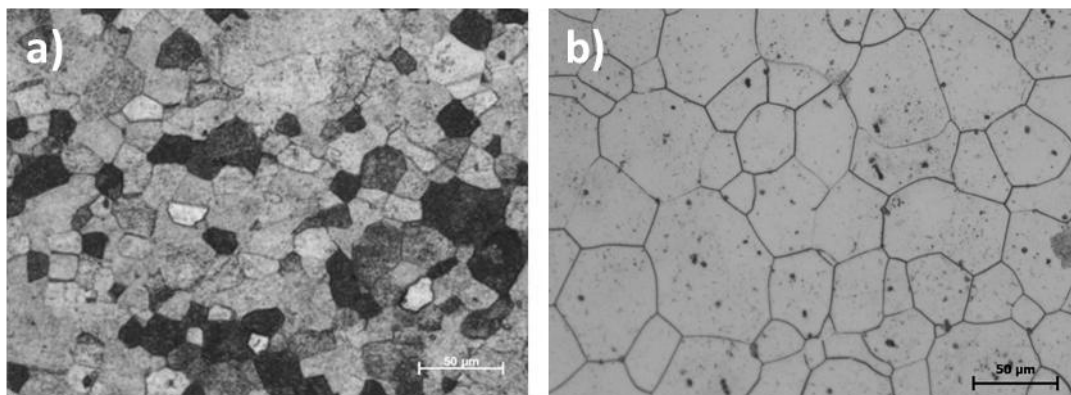
3. RESULTS AND DISCUSSION

The result of the chemical composition of 409 and 439 ferritic stainless steels (SS) obtained by the technique of X-ray fluorescence spectrometry (XRF), is as follows.

Table 1. Chemical composition of 409 and 439 SS.

Material	Concentration of elements, % wt											
	Fe	Cr	Si	Mn	Ti	Ni	V	P	Cu	Mo	S	Nb
SS 409	88.01	10.73	0.34	0.34	0.24	0.14	0.05	0.025	0.11	0.016	0.02	**
SS 439	80.96	17.33	0.43	0.5	0.19	0.19	0.08	0.056	0.12	0.014	0.028	0.192

In Figure 1, can be observed the microstructures of 409 and 439 stainless steels etched with reagent Vilella. It is shown the ferritic structure with smaller grain size for the stainless steel 409 than for steel 439.

**Figure 1.** Microstructure of ferritic stainless steel. a) 409 and b) 439

In cyclic polarization curves, the potential is plotted against the logarithm of the current. In these graphs can identify the mechanism of corrosion of stainless steel, where the anodic and cathodic reactions of the system were analyzed. In the cyclic polarization curves, is described the increment on the branch anodic current. When graphics makes a return inside of itself, it is said that corrosion system hysteresis is occurring and pitting will happen.

Cyclic potentiodynamic polarization comparative curves for 409 stainless steel in three different medium are shown in figure 2, where it can be observed the positive hysteresis for medium as water and brine, in opposite to the sulfuric acid case. In the corresponding curve for sulfuric acid electrolyte, has a negative hysteresis (which rejects pinholes formation).

In this technique is swept an applied anodic potential from corrosion potential, E_{corr} , up to the potential at which the reverse current value i_{Rev} is reached. This potential is called reverse potential E_{rev} . At this point the potential is reversed until crossing the anodic curve; that potential is called protection potential E_{prot} . From pitting potential E_{np} until E_{rev} , there is the area where pits nucleate and propagate. However, between the potential E_{np} and E_{prot} there is an area where no new pits nucleate, but those present, they can still spread. Below E_{prot} , no pits will nucleate or spread [10].

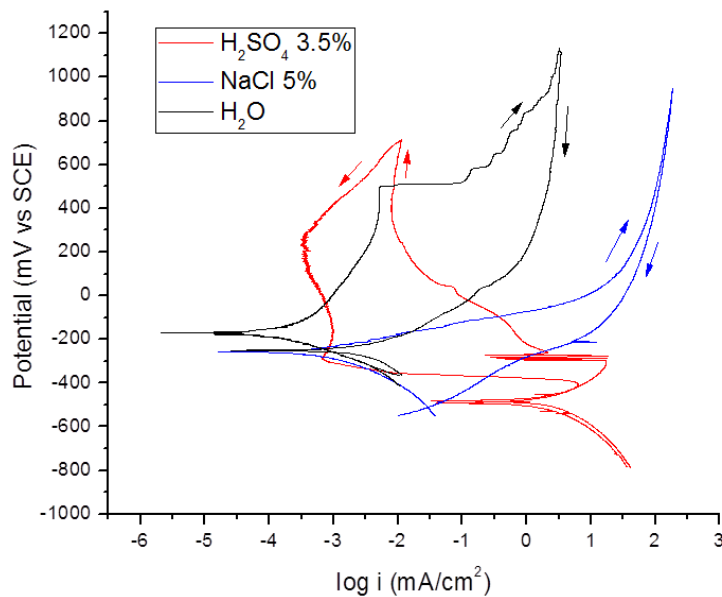


Figure 2. Cyclic potentiodynamic polarization curves in different solutions for 409 SS.

In the case of H_2SO_4 solution has a higher current density of approximately 0.5 mA/cm^2 , and its anodic branch initially displays an activation state behavior followed by passivation to a corrosion current density of 1.5 mA/cm^2 approx.

In the solution of NaCl has a E_{corr} of -280 mV and a current density of about $3 \times 10^{-3} \text{ mA/cm}^2$. The behavior observed in this solution is basically activation.

The water nobler E_{corr} shows, as well as, the corrosion current density of E_{corr} . This solution tends to a passivation, approximately 3 mA/cm^2 and a E_{np} to -500 mV until E_{rev} , across to the cathodic branch.

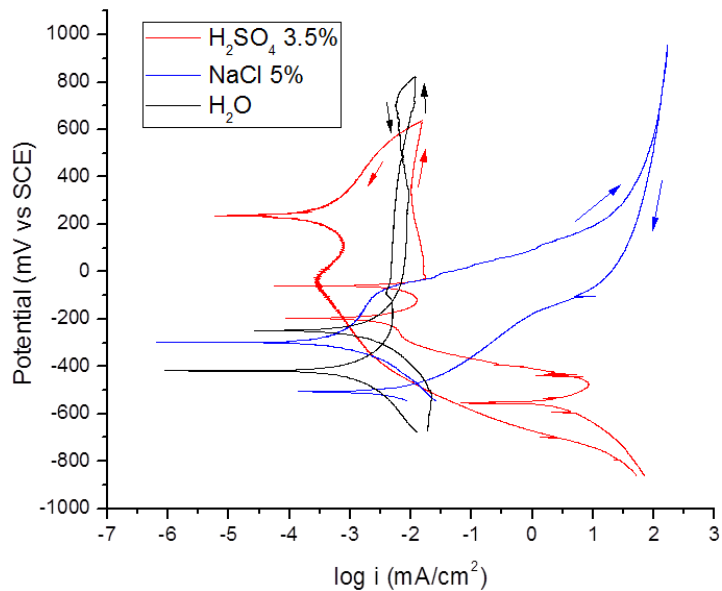


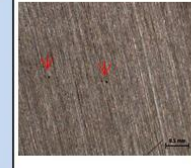
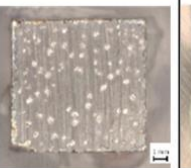
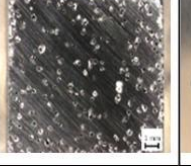
Figure 3. Cyclic potentiodynamic polarization curves in different solutions for 439 SS.

In the above figure, it is able to see the electrochemical behavior of 439 stainless steel in the test solutions. Only in the solution of sodium chloride is presented the typical behavior of pitting corrosion. In water and sulfuric acid solutions the hysteresis returns inside, indicating that the pitting mechanism will not be developed.

The H_2SO_4 solution appears similar to 409 stainless steel behavior, however with a lower current density of approximately 0.3 mA/cm^2 , and the passivation is faster, at a current density of 1mA/cm^2 approx.

In the case of NaCl solutions and water have almost the same corrosion current density of $5 \times 10^{-3} \text{ mA/cm}^2$. This material in NaCl , unlike 409SS, tends to exhibit E_{np} passivation at -100 mV and has a crossing until the cathodic branch (E_{pp}). The water has a passivation state a corrosion current density of $2 \times 10^{-2} \text{ mA/cm}^2$.

Table 2. Surface state of the samples after the electrochemical tests.

Materials	Electrolyte		
	H_2O	NaCl	H_2SO_4
409 SS			
439 SS			

On table 2 the samples conditions are shown after the electrochemical cyclic polarization curves tests. Can be appreciated the pitting corrosion damage in sodium chloride solution, that were reflected in corresponding polarization curves.

In the remaining samples the corrosion activity was taken across the entire surface, being in sulfuric acid tests the most affected.

The electrochemical noise provides information about the reaction kinetics, i.e. the corrosion rate; being possible to identify the type of corrosion either as uniform, generalized or localized. It is also possible to get information about the reaction mechanisms [11].

In the current time series is observed increased corrosion activity by the 409 stainless steel, which tends to increase at 1200 seconds of the trial and coupled with this can be appreciated transients indicating localized corrosion activity, however these transients are of low amplitude and frequency. This behavior is consistent with that shown in the polarization curves and observed in photographs. In the case of 439 stainless steel is characterized with a uniform corrosion behavior.

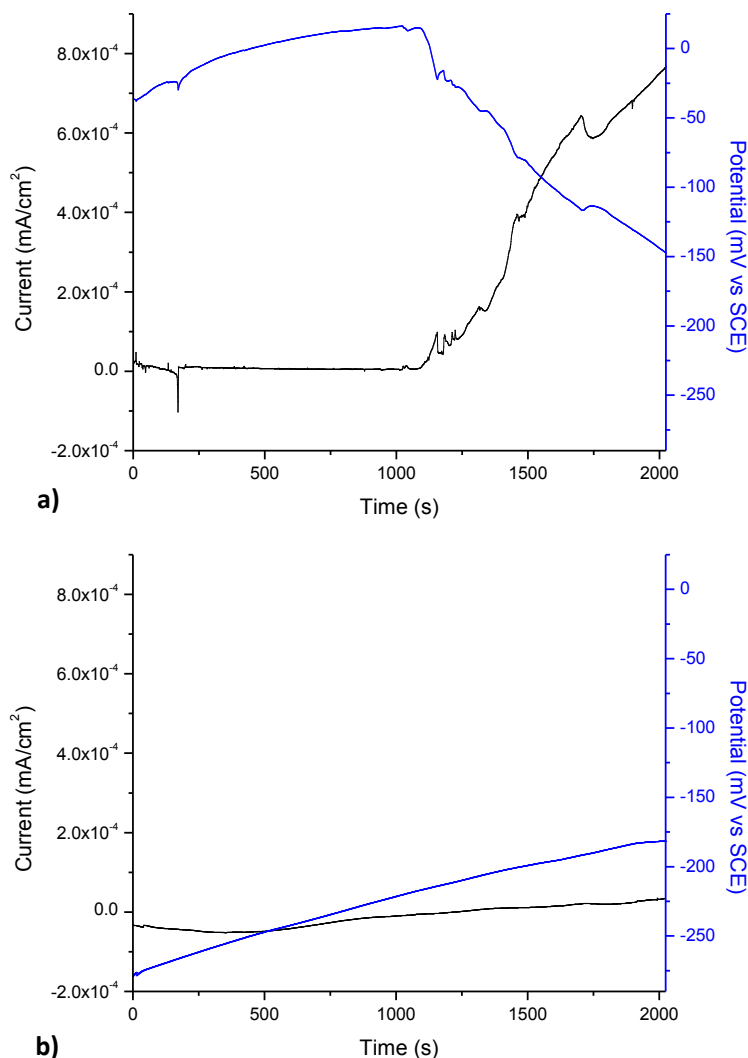


Figure 4. The current and potential time series for electrochemical noise measurements a) 409 and b) 439 stainless steels in H₂O.

In the case of brine time series, figure 5, is observed by the 409 stainless steel a trend towards active potentials and distinguishable current transients followed by fluctuations of low frequency that set the evident preference for pitting after short periods of passivation. In the case of 439 steel are identified transients in the same manner and indicate localized activity on the material surface, sometimes with passivation and depassivation periods and prone to negative potentials. These graphs are characteristic of corrosion pitting process.

Finally, the time series corresponding to the sulfuric acid has low amplitude fluctuations clearly indicating the preference of the material to undergo a uniform corrosion type. The order of magnitude in relation to those presented in the previous two solutions is significantly higher, which reinforces what is observed in the graphs of cyclic polarization, in spite of, this material does not present a pitting type, but a significant activity occurs for generalized corrosion and it is evidenced at high frequencies in the time series.

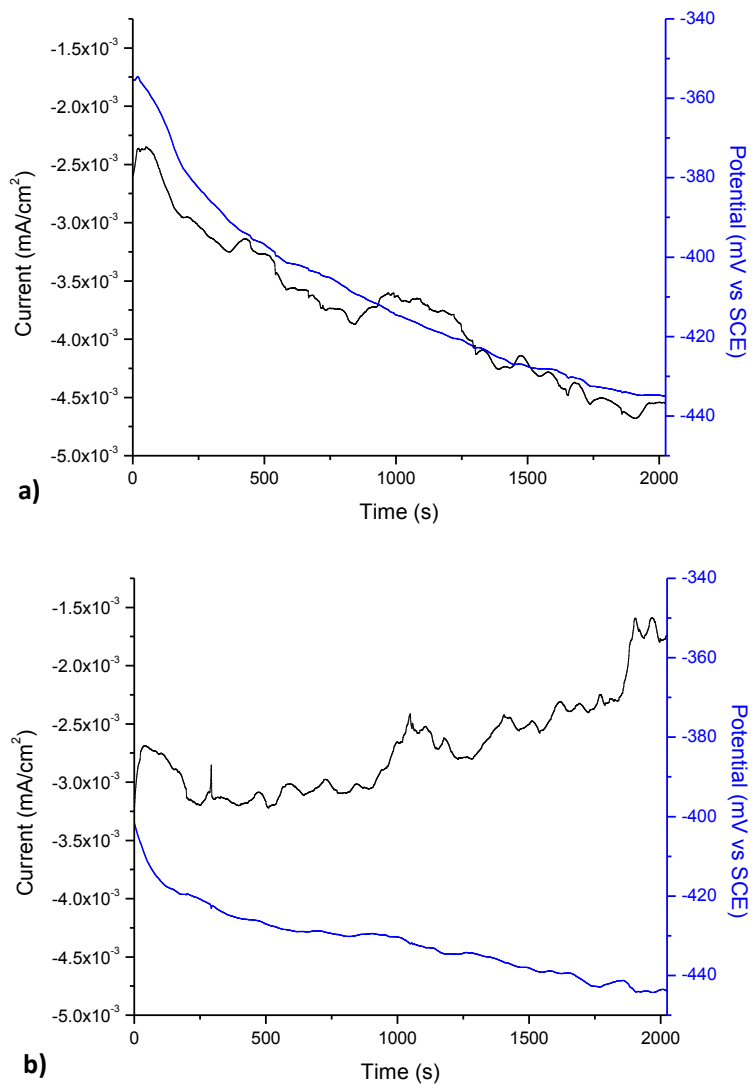


Figure 5. The current and potential time series for electrochemical noise measurements a) 409 and b) 439 stainless steels in NaCl 5%.

The potential time series tends to remain constant at negative potentials [11-12]. For subsequent statistical analysis of current and potential time series, which includes the location index (IL), making reference to Kelly, Inman and Hudson, the calculation of the noise resistance, Rn, (Equation 1) was carried out with the ratio of the standard deviations of the measured potential and current [13-15]:

$$Rn = \frac{\sigma E}{\sigma I} \quad \text{Equation 1.}$$

The location index (Equation 2), is a parameter that evaluates the variation in current noise and compares the average value was calculated by the ratio of the current standard deviation and root mean square current according to [16-17]:

$$IL = \frac{\sigma I}{I_{RMS}}$$

Equation 2

In Table 3 are presented the parameters obtained from statistical analysis results of the electrochemical noise signals for ferritic 409 and 439 stainless steels in electrolytes under study. The type of corrosion that occurs is uniform, localized and mixed.

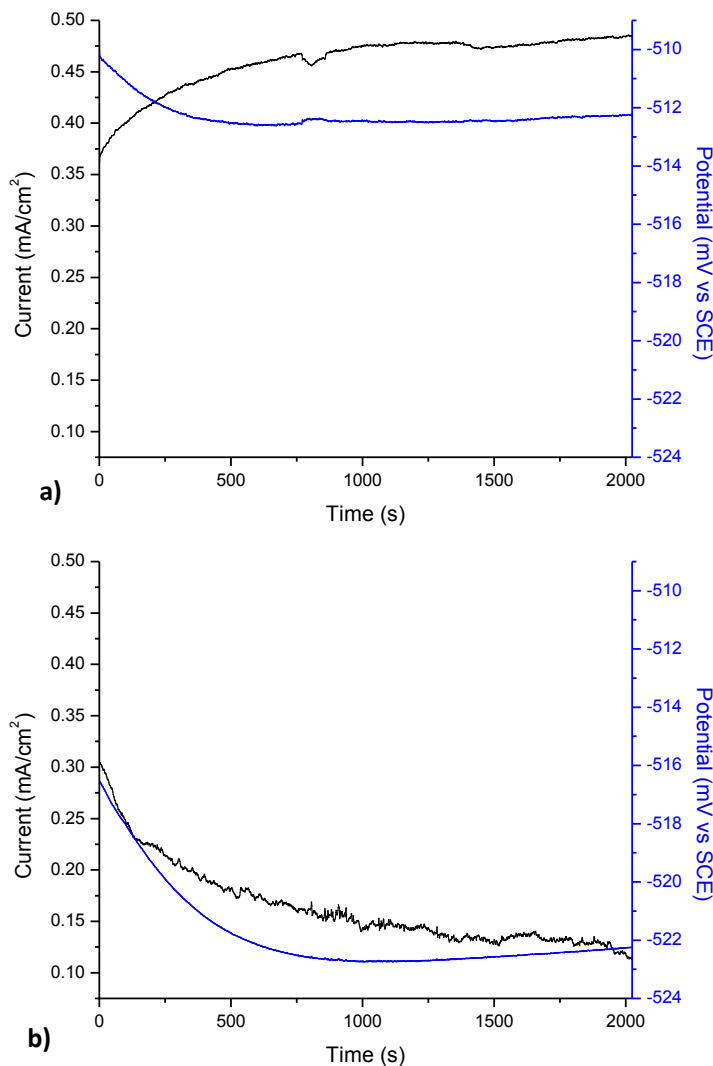


Figure 6. The current and potential time series for electrochemical noise measurements a) 409 and b) 439 stainless steels in H_2SO_4 3.5%

The stainless steels should be used with caution in environments that contains sodium chloride. The chloride ions, Cl^- , increased active corrosion reactions and hence increase in corrosion magnitude (18). The action of aggressive ions, especially chloride ions Cl^- , which by increasing its concentration increases the pitting [19-20], cause passive films are susceptible to localized breakdown, resulting in a

rapid dissolution of the metal [21] mainly in places where there are heterogeneities, causing localized corrosion, mainly pitting corrosion as stainless steels. [9,22]. Localized corrosion is a serious problem for stainless steels when they are exposed to acid solutions.

The sulphuric acid is oxidising when concentrated but is reducing at low and 'intermediate' concentrations. The mechanism of corrosion by the presence of an acidic solution causes the passivation film is broken and generated uniform corrosion. The principal active agent for corrosion in aqueous solutions of sulfuric acid is the SO_4^{2-} anion, which participates in anodic and cathodic reactions during corrosion process, and hydrogen atoms adsorbed on the surface of metal have a depassivating effect that increase the corrosivity of the acid [23-24].

Table 3. Parameters of electrochemical noise.

Material	Electrolyte	Rn (mΩ·cm ²)	Icorr (mA/cm ²)	Corrosion rate (mm/year)	Location index	Corrosion type
SS 409	water	195810	1.33×10^{-04}	1.5×10^{-03}	0.09	mixed
	NaCl 5%	35338	7.33×10^{-04}	8.29×10^{-03}	0.54	localized
	Sulfuric acid 3.5%	93.189	0.279	3.12	0.0013	uniform
SS 439	water	519550	5.021×10^{-05}	5.639×10^{-04}	0.04	mixed
	NaCl 5%	55231	4.72×10^{-04}	5.30×10^{-03}	0.36	localized
	Sulfuric acid 3.5%	66.855	0.3889	4.35	0.0054	uniform

In Figure 7, are the graphs for the corrosion rates gotten for the studied steels in different testing solutions.

The sulfuric acid solution caused greatest damage to the stainless steel samples, and mostly to steel 439, presenting a corrosion rate of 4.35 mm/year.

In water solutions and sodium chloride the 439 stainless steel presented a better performance, with similar values of corrosion rate of about 1.33×10^{-04} mm/year. The steel 409 has a difference in the corrosion values of one order of magnitude between water and NaCl.

The corrosion rate was calculated in terms of the corrosion current density, Icorr, and in accordance with ASTM G102-89 [25-27]; this calculation was done according to Equation 3.

$$\text{corrosion rate} = \frac{C\omega i_{corr}}{\rho} \quad \text{Equation 3.}$$

Where C is a conversion factor (3.27 mm·g/mA·cm·year), ω is the equivalent weight (g), ρ is the material density (g/cm³), and icorr is the corrosion current density (mA/cm²).

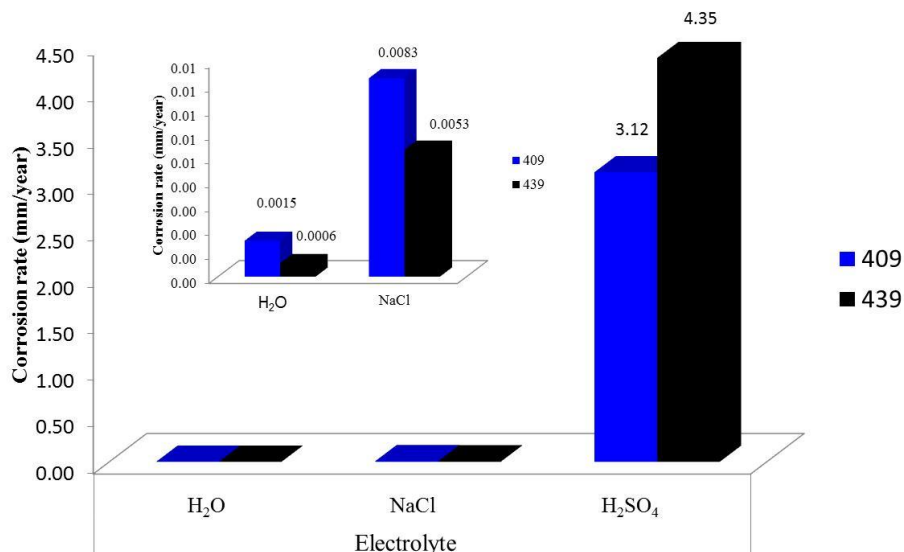


Figure 7. Corrosion rates of 409 and 439 SS in different electrolyte.

4. CONCLUSIONS

- Electrochemical tests showed preferential pitting in the sodium chloride solution for both materials. Sulfuric acid is one of the electrolytes presented greatest corrosion rate, although its mechanism of corrosion is not for steel pitting, but for general corrosion.
- The transients presented in all time series of potential and current for electrochemical noise measurements show repeatability and are characteristic of pitting nucleation or metastable pitting.
- According to obtained results of the statistical analysis of current and potential time series from electrochemical noise, for ferritic 409 and 439 stainless steels in electrolytes under study, the type of corrosion that occurs is uniform, localized and mixed.
- The stainless steels should be used with caution in environments that contains sodium chloride and sulfuric acid.
- Cyclic polarization curves and electrochemical noise, both techniques have a consistent result with the mechanism of corrosion as well as their electrochemical parameters.
- The ferritic 439 stainless steel performs better corrosion resistant than 409 SS in water and sodium chloride environments, but in sulfuric acids the corrosion rate was substantially greater.

ACKNOWLEDGEMENTS

The authors wish to thank the Academic Group UANL-CA-316.

References

1. N. Renaudot, PO. Santacreu, J. Ragot, JL Moiron, R. Cozar R, Pédarré and A. Bruyère 430LNb—a new ferritic wire for automotive exhaust applications. SAE Technical Paper Series, 2000-01-0314

2. J. Honeycombe, TG. Gooch, *Br Corros J.*, 18 (1983) 25–34
3. L. Faivre, P-O Santacreu, J. Leseux, *Tecnol Metal Mater.*, 8 (2011) 24–30
4. K. Inui, T. Noda, T. Shimizu and M. Nagata, Development of the ferritic stainless steel welding wire providing fine grain microstructure weld metal for the components of automotive exhaust system. SAE Technical Paper Series, (2003) 01- 979
5. F. J. Rodríguez, “Técnicas Electroquímicas de Corriente Directa para la Medición de la Velocidad de Corrosión: Resistencia a la Polarización” Fundamentos Técnicas Electroquímicas(2002). Edit J. Genescá UNAM.
6. Ma. Fong-Yuan, Corrosive Effects of Chlorides on Metals. Pitting Corrosion Intech Open, (2012). 139-178.
7. A.A. Khedr, S.H. Sanad, K.M. El-Sobki, *Surf. Technol.*, 23 (1984) 151-158
8. ASTM G5-13 “Standard Reference Test Method for Making Potentiodynamic Anodic Polarization Measurements” American Society for Testing Materials Annual, Book of ASTM Standards, (2013) Vol. 03.02 West Conshohocken USA.
9. ASTM G199–09 “Standard Guide for electrochemical Noise Measurements” American Society for Testing Materials Annual, Book of ASTM Standards, (2014) Vol. 03.02 West Conshohocken USA.
10. Z. Szklarska-Smialowska. Pitting Corrosion of Metals, National Association of Corrosion Engineers, Houston, Texas, EE.UU, (1986) p. 1,70, 375, 377-400.
11. J.A. Cabral M., J. Barcenas S., C.A Poblano, *Int. J. Elechochem Sci.*,8 (2003) 564 -577.
12. F. H. Estupiñán L.F., F. Almeraya C.F., R. Bautista M. *Int. J. Elechochem Sci.*, 6 (2011) 1785-1796
13. P.A. Cottis, S. Turgoose, “Electrochemical Impedance and Noise” Corrosion Testing Made Easy. (1999) Series NACE, Houston TX, USA.
14. F. Barragán, R. Guardián, C. Menchaca, I. Rosales, J. Uruchurtu, *Int. J. Electrochem. Sci.*, 5 (2010) 1799 – 1809.
15. A.Legat, V. Dolecek, *J. Electrochem. Soc.*, 142, (1995) 1851.
16. J.M. Sanchez-Amaya, RA. Cottis and F.J. Botana, *Corros Sci.*, 47 (2005) 3280.
17. J. R. Kearns, J. R. Scully, P. R. Roberge, D.L. Reichert, J. L. Dawson. *Electrochemical Noise Measurement, for Corrosion Applications, STP1277*, (1996) ASTM
18. V. Anbazhagan and R. Nagalakshmi, *Weld Res J.*, 23 (2002) 25–37.
19. C.A. Loto and R.T. Loto, *Int. J. Electrochem. Sci.*, 7 (2012) 11011 - 11022.
20. O. A. Hazzazi, A. M. Zaky, Mohammed A. Amin and Sayed S. Abd El Rehim, *Int. J. Electrochem. Sci.*, 3 (2008) 489-508.
21. K. Darowicki, A. Mirakowski, S. Krakowiak, *Corros Sci.*, 45 (2003) 1747-1756.
22. A.Pardo, M.C. Merinoa, A.E. Coyb, F. Viejob, R. Arrabalb and E. Matykinab, *Corros Sci.*, 50 (2008) 1796-180.
23. A.K. Mindyuk, E.I. Svist, O.P. Savitskaya, L.N. Petrov, Z.M. Gutman, *Mater. Sci.*, 3 (2003) 157-164.
24. M. Abdallah, *Mater. Chem. Phys.*, 82 (2003) 786-792.
25. J.A. Cabral, J. Barceinas, C.A. Poblano, G. Pedraza, *Int. J. Electrochem. Sci.*, 8 (2013) 564 - 577.
26. M. Stern and A.L. Geary, *J. Electrochem. Soc.*, 104 (1957) 56.
27. ASTM-G102, Standard Practice for Calculation of Corrosion Rates and Related Information from Electrochemical Measurements, ASTM International, (1999). West Conshohocken, PA.